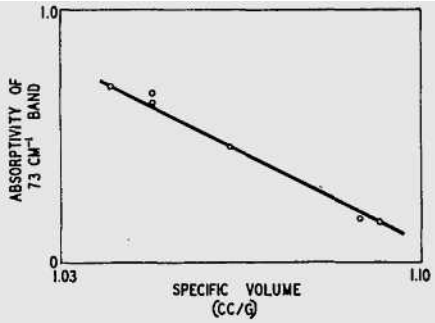

FIG. 1. Absorptivity of 73 cm^{-1} band in polyethylene and olefin copolymers vs their specific volume.

Sample cells of polyethylene are sometimes used in the far-infrared region, below 200 cm^{-1}. Identification of the 73 cm^{-1} band with polyethylene indicates that caution should be taken when this region is investigated using polyethylene cells, particularly since the band is stronger in the high-density polymers which are more desirable for cells because of their better mechanical strength and chemical properties.

[1] R. V. McKnight and K. D. Möller, J. Opt. Soc. Am. 54, 132 (1964).

Fish Eye Lens

KENRO MIYAMOTO*
Institute of Plasma Physics, Nagoya University, Nagoya, Japan
(Received 19 February 1964)

A LENS which covers a hemispherical field ($2\omega=180°$) is usually called a fish eye lens. This lens is not an extension of a wide angle lens. It has inherent large distortion because it is not possible to form an image of a hemispheric field on a plane without distortion. The classical example of this type of image formation is a fish eye under water. Wood[1] took a photograph with a pinhole camera filled with water [Fig. 1(a)]. Bond[2] substituted a hemispheric lens with a pupil at the center of curvature [Fig. 1(b)] in place of the water in the pinhole camera. However, this lens has a large Petzval sum. The field curvature was greatly improved by

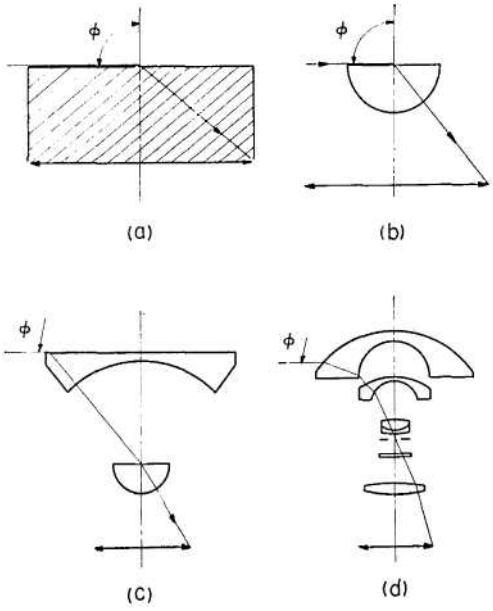

FIG. 1. Development of fish eye lens.

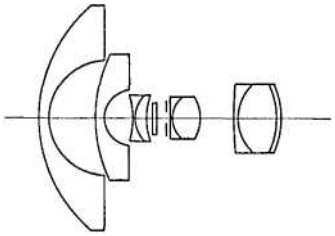

FIG. 2. A fish eye lens with corrected color aberration.

adding a diverging meniscus lens before the hemisphere lens [Hill,[3] Fig. 1(c)[4]], which is a prototype of the present fish eye lenses. Fish eye lenses have also been improved by Schultz[5] [Fig. 1(d)], Merté,[6] and recently by van Heel.[7]

However, large lateral color aberration cannot be corrected by these lenses, and color filters must be employed in order to take photographs. The lateral color aberration can be corrected by adding a doublet (positive flint glass lens and negative crown glass lens) before the pupil as is shown in Figs. 2 and 3 (see also Table I). Now all the wavelengths to which the photographic material is sensitive can be utilized and color photographs can also be taken. When the fish eye lens is pointed toward the zenith, the image of the subject of principal interest may appear at the edge of the field more frequently than at the center. Therefore correction of aberrations at the edge is very important.

The fish eye lens has inherent distortion; this distortion should not be considered as an aberration but as a result of projection of a hemisphere on a plane. Let the angle of an incident ray from an infinite object be ϕ and the coordinates of the image be (r',θ). The following projections are considered in this section:

$$r'=f\tan\phi, \tag{1}$$

$$r'=2f\tan(\phi/2), \tag{2}$$

$$r'=f\phi, \tag{3}$$

$$r'=2f\sin(\phi/2), \tag{4}$$

where f is the focal length.

Projection 1 is that of camera lenses. Projection 2 is called stereographic projection. From Eq. (2), we have

$$dr'=f(\cos\phi/2)^{-2}d\phi, \tag{2'}$$
$$r'd\theta=f(\cos\phi/2)^{-2}(\sin\phi d\theta).$$

This result shows that a small circle on a hemisphere having its center at the lens is projected as a circle on the image plane, but the diameter of the image of a circle at the horizon, $\phi=90°$, is twice as large as the image of an equally large circle at the pole, $\phi=0°$. This projection is very similar to our psychological percept of whole sky.[3]

Projection 3 is called equidistance projection. It is represented at 3 in Fig. 4. This is preferable for measurement of zenith angles and azimuth angles. The effect of error of lens position is small, and the linear relation of r' and ϕ is convenient to analyze. An attempt was made to accomplish equidistance projection with the fish eye lens shown in Fig. 2. However, the image of a small circle

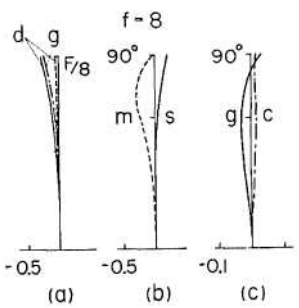

FIG. 3. Aberration curves of fish eye lens shown in Fig. 2. Curves *a* show spherical aberration of *d* and *g* lines and sine condition of *d* line, dotted. Curves *b* show astigmatism, and curves *c* show lateral color aberration for *c* and *g* lines.

TABLE I. Lens data of fish eye lens shown in Fig. 2. r, d, n_d, and ν_d are radius of curvature, distance, index of refraction (d line), and Abbe number, respectively.

r	d	n_d	ν_d
		1	
47.91	2.8	1.5168	64.2
18.85	15.2	1	
48.4	2.4	1.4883	70.4
8.88	9.6	1	
−36.16	0.8	1.4883	70.4
10.21	3.6	1.7865	26.0
37.0	2.0	1	
∞	1.2	1.5174	59.0
∞	4.0	1	
3078.0	0.8	1.7865	26.0
7.6	8.8	1.7445	45.0
−13.0	10.4	1	
110.0	1.6	1.7865	26.0
14.17	12.0	1.7023	41.0
−32.0	1.5	1.6686	41.9
−26.98		1	

is not a circle because

$$\left.\begin{aligned} dr' &= f d\phi, \\ r'd\theta &= f(\phi/\sin\phi)(\sin\phi d\theta). \end{aligned}\right\} \tag{3'}$$

Projection 4 may be called equisolid angle projection, because the element of solid angle $d\Omega$ is expressed by

$$d\Omega = \sin\phi d\phi d\theta = (1/f^2)r'dr'd\theta = (1/f^2)dS', \tag{4'}$$

and the solid angle Ω is proportional to the corresponding area S' in the image plane. This projection is convenient for measuring the percentage of the sky covered by clouds, or obstructed by buildings. For the equidistance projection, we have

$$d\Omega = (1/f^2)[\sin(r'/f)/(r'/f)]dS'. \tag{3''}$$

When the radiant flux from a small area dS of the object plane (r,θ) in a small solid angle $d\Omega$ in the direction ϕ is concentrated to the small area dS' of the image plane (r',θ') within the solid angle $d\Omega'$ of the direction ϕ', then the following relation holds:

$$n^2\cos\phi d\Omega dS = n'^2\cos\phi' d\Omega' dS', \tag{5}$$

where n and n' are the indices of refraction of object and image space, respectively. When the radiance of object is N, the radiant flux density W is

$$\begin{aligned} W &= \int N\cos\phi' d\Omega', \\ &= \int N(n/n')^2\cos\phi(dS/dS')d\Omega'. \end{aligned} \tag{6}$$

Let the area of entrance pupil and the distance of object plane and entrance pupil be a and l (see Fig. 5). When equidistance projection is employed we have

$$r' = f\phi, \quad r = l\tan\phi. \tag{7}$$

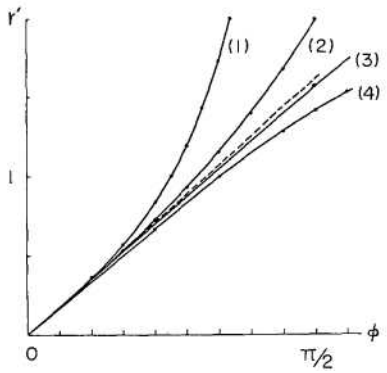

FIG. 4. Curves of various projections: (1) ordinary projection, (2) stereographic projection, (3) equidistance projection, (4) equisolid angle projection.

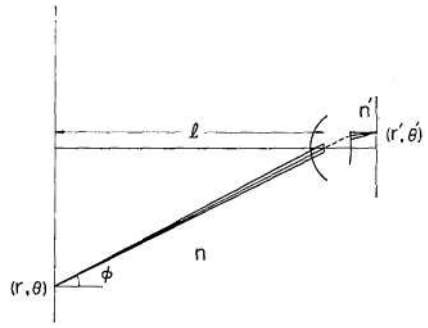

FIG. 5. Explanation of notations used in Eqs. (5) and (6).

If $\sqrt{a} \ll l$, then

$$\begin{aligned} &\Delta\Omega \sim a\cos\phi/(l/\cos\phi)^2, \\ &dS/dS' = rdrd\theta/r'dr'd\theta' = (l^2\tan\phi/\cos^2\phi)/f^2\phi, \end{aligned} \tag{8}$$

and

$$\begin{aligned} W &\sim (n/n')^2 N\cos\phi\Delta\Omega(dS/dS'), \\ &= (n/n')^2 N(a\cos\phi/f^2)(\sin\phi/\phi). \end{aligned} \tag{9}$$

For the fish eye lens shown in Fig. 2, $a\cos\phi$ is nearly constant and W is finally reduced to $W = (n/n')^2 N(\pi/4F^2)(\sin\phi/\phi)$, where F is the f/number. Therefore, the radial flux density is relatively uniform, as compared to ordinary lenses, which obey the $\cos^4\phi$ law.

* This work was done when the author was in Nippon Kogaku K.K. (Japan Optical Industry Company).

[1] R. W. Wood, *Physical Optics* (Macmillan and Company, Ltd., London, 1919), p. 67.
[2] W. N. Bond, Phil. Mag. 44, 999 (1922).
[3] R. Hill, *Proceedings of the Optical Convention* (1926) 878.
[4] C. Bech, J. Sci. Instr. 2, 135 (1925).
[5] H. Schulz, D. R. Patent No. 620538 (1932).
[6] W. Merté, D. R. Patent No. 672393 (1935).
[7] A. C. S. van Heel *et al.*, U. S. Patent No. 2947219 (1960).

Continuous Recording of Raman Spectra Excited with the He–Ne Gas Laser

J. A. KONINGSTEIN AND R. G. SMITH
Bell Telephone Laboratories, Incorporated, Murray Hill, New Jersey 07971

(Received 27 April 1964)

CONTINUOUS photoelectric recording of Raman spectra excited by the 6328 Å line of a He–Ne gas laser has recently been reported by Porto and Leite.[1] In their experiments the Raman cell was placed inside the laser cavity. We have photoelectrically recorded Raman scattering from liquids using cells external to the

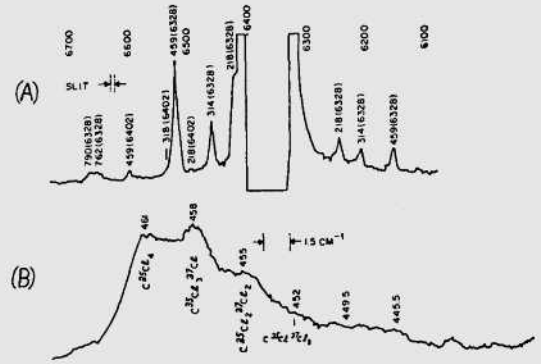

FIG. 1. (a) The Raman spectrum of CCl_4 excited by the 6328 and 6401 Å lines of a He–Ne gas maser. Time constant, 3.2 sec; speed, 40 Å/min; slit, 200 $\mu \cong 3.2$ Å. (b) The 459 cm^{-1} band of CCl_4 under higher resolution: Time constant, 32 sec; speed, 2 Å/min; slit, 125 $\mu \cong 1.5$ cm^{-1}.